THE JOURNAL OF BIOLOGICAL CHEMISTRY VOL. 288, NO. 19, pp. 13236–13242, May 10, 2013
Published in the U.S.A.

Major Histocompatibility Complex (MHC) Class II-Peptide Complexes Arrive at the Plasma Membrane in Cholesterol-rich Microclusters*[S]

Received for publication, December 5, 2012, and in revised form, March 4, 2013 Published, JBC Papers in Press, March 26, 2013, DOI 10.1074/jbc.M112.442640

Berta Bosch[‡], Erica L. Heipertz[‡], James R. Drake[§], and Paul A. Roche[‡1]

From the [‡]Experimental Immunology Branch, NCI, National Institutes of Health, Bethesda, Maryland 20892 and the [§]Center for Immunology and Microbial Disease, Albany Medical College, Albany, New York 12208

Background: Antigen-specific CD4 T cells are activated by small numbers of antigenic peptide-MHC class II (pMHC-II) complexes on dendritic cells (DCs).
Results: Newly generated pMHC-II complexes are present in small clusters on the DC surface.
Conclusion: pMHC-II clusters permit efficient T cell activation.
Significance: The appearance of clustered pMHC-II reveals the organization of the T cell antigen receptor ligand on the DC surface.

Dendritic cells (DCs) function by stimulating naive antigen-specific CD4 T cells to proliferate and secrete a variety of immunomodulatory factors. The ability to activate naive T cells comes from the capacity of DCs to internalize, degrade, and express peptide fragments of antigenic proteins on their surface bound to MHC class II molecules (MHC-II). Although DCs express tens of thousands of distinct MHC-II, very small amounts of specific peptide-MHC-II complexes are required to interact with and activate T cells. We now show that stimulatory MHC-II I-A^k-$HEL_{(46-61)}$ complexes that move from intracellular antigen-processing compartments to the plasma membrane are not randomly distributed on the DC surface. Confocal immunofluorescence microscopy and quantitative immunoelectron microscopy reveal that the majority of newly generated MHC-II I-A^k-$HEL_{(46-61)}$ complexes are expressed in sub-100-nm microclusters on the DC membrane. These microclusters are stabilized in cholesterol-containing microdomains, and cholesterol depletion inhibits the stability of these clusters as well as the ability of the DCs to function as antigen-presenting cells. These results demonstrate that specific cohorts of peptide-MHC-II complexes expressed on the DC surface are present in cholesterol-dependent microclusters and that cluster integrity is important for antigen-specific naive CD4 T cell activation by DCs.

Antigen-specific CD4 T cells are stimulated by the engagement of their T cell receptor (TCR)[2] with antigen-bearing MHC class II molecules (MHC-II) present on the surface of professional antigen-presenting cells (APCs) (1). MHC-II bind antigenic peptides generated by proteolysis of internalized proteins in intracellular lysosome-like antigen-processing compartments in APCs (2). The most relevant APC for stimulating naive CD4 T cells is the dendritic cell (DC). Following peptide binding onto MHC-II, the newly formed peptide MHC-II complexes (pMHC-II) leave these intracellular compartments and move to the plasma membrane in tubular endosomes (3, 4). These endosomes dock onto and fuse with the plasma membrane, thereby delivering pMHC-II to the DC surface, where they potentially interact with pMHC-II-specific TCRs present on naive CD4 T cells.

MHC-II are constitutively synthesized in resting DCs, and in these cells, a diverse repertoire of pMHC-II is generated that reflects the general composition of self-peptides present in antigen-processing compartments. After endocytosis of a pathogen that contains a DC-stimulating ligand (such as bacterial lipopolysaccharide (LPS) or double-stranded viral RNA), the DC transiently up-regulates macropinocytosis (5) and MHC-II synthesis (6), coordinated processes that likely poise the DC to generate specific pMHC-II required to activate antigen-specific T cells. Although this process does *enrich* the DC surface with antigen-specific pMHC-II, the number of specific pMHC-II required to activate CD4 T cells is generally less than 500 complexes per cell and thus represents a very small fraction of the total pool of MHC-II on the DC surface (7, 8).

We have been interested in understanding how APCs expressing relatively small amounts of specific MHC-II efficiently interact with antigen-specific T cells. We and others have proposed that the association of distinct proteins with cholesterol/sphingolipid-rich lipid microdomains, termed lipid rafts, serves to concentrate them in these microdomains and increases their local density on the cell surface (9, 10). MHC-II associates with lipid raft membrane microdomains, and we (and others) have shown that lipid raft association of MHC-II on the surface of APCs is important for their ability to stimulate

* This work was supported, in whole or in part, by National Institutes of Health Grant AI-065773 (to J. R. D.) as well as the Intramural Research Program of the National Institutes of Health (to P. A. R.).
[S] This article contains supplemental Figs. 1 and 2.
[1] To whom correspondence should be addressed: National Institutes of Health; Bldg. 10, Rm. 4B36, Bethesda, MD 20892. Tel.: 301-594-2595; Fax: 301-435-7923; E-mail: paul.roche@nih.gov.
[2] The abbreviations used are: TCR, T cell receptor; MHC-II, MHC class II molecule(s); pMHC-II, peptide-MHC-II complex(es); APC, antigen-presenting cell; DC, dendritic cell; HEL, hen egg lysozyme; MCD, methyl-β-cyclodextrin; HBSS, Hanks' balanced salt solution; PFA, paraformaldehyde; CFSE, carboxyfluorescein succinimidyl ester.

antigen-specific CD4 T cells (9–12). However, the mechanism by which small numbers of specific pMHC-II can "find" each other on the plasma membrane and concentrate in microdomains has remained elusive.

We now show that specific pMHC-II generated in DCs arrive at the plasma membrane in microclusters that are visible by conventional immunofluorescence microscopy as well as by immunoelectron microscopy. Perturbation of plasma membrane microdomains by cholesterol extraction using methyl-β-cyclodextrin (MCD) results in the dissolution of these clusters and inhibits antigen-specific CD4 T cell proliferation when the DCs are pulsed with small amounts of antigen but not when the DCs are pulsed with large amounts of antigen. These data show that newly formed pMHC-II appear at the DC surface in microclusters that are stabilized by membrane cholesterol, thereby allowing the concentration of relatively small amounts of specific pMHC-II that are required to activate CD4 T cells.

EXPERIMENTAL PROCEDURES

Cells and Reagents—DCs were obtained by culturing bone marrow cells from B10.BR mice in GM-CSF (PeproTech) for 6 days using protocols described previously (13). These bone marrow-derived DCs were either untreated or pulsed with HEL protein antigen (Sigma) for 12 h. At day 7, the antigen was removed, and the cells were activated by incubation with 1 μg/ml LPS (Sigma) for an additional 12 h. Naive CD4 T cells from I-A^k-$HEL_{(46-61)}$ complex-specific 3A9 TCR transgenic mice were obtained from spleen/lymph nodes by negative selection using a MACS mouse CD4 T cell isolation kit (Miltenyi Biotec). All mice were cared for in accordance with National Institutes of Health guidelines with the approval of the NCI Animal Care and Use Committee. Two different I-A^k-$HEL_{(46-61)}$ complex-specific mAbs were used in this study: mAb Aw3.18.14 (14) was from the American Type Culture Collection (ATCC), and mAb C4H3 (15) was a gift from Ron Germain, National Institutes of Health, Bethesda, MD. The mouse ICAM-1 mAb (clone YN1/1.7.4) was purchased from SouthernBiotech. Sulfo-NHS-biotin was from Pierce, MCD was from Sigma-Aldrich, Alexa Fluor 488-labeled cholera toxin B subunit was from Molecular Probes, colloidal gold-conjugated goat antibodies were from Electron Microscopy Sciences, and Alexa Fluor-labeled secondary antibodies, Alexa Fluor 546-labeled streptavidin, and CFSE were from Invitrogen.

Cell Surface Biotinylation and Cholesterol Depletion—Plasma membrane proteins of DCs were biotinylated on ice according to procedures described previously (16). To deplete cholesterol, cells were treated with 10 mM MCD in HBSS for 10 min at 37 °C and washed twice in ice-cold HBSS. After cholesterol depletion, cells were analyzed immediately for total cholesterol content using an Amplex Red Cholesterol Assay kit (Molecular Probes), stained live (on ice) for confocal immunofluorescence microscopy analysis, or fixed with 2% paraformaldehyde (PFA) in HBSS prior to culture with antigen-specific naive CD4 T cells. In some experiments, the MCD-treated and PFA-fixed cells were assayed for expression of I-A^k-$HEL_{(46-61)}$ complexes by FACS using mAb C4H3. This mAb was used because control experiments revealed that mAb Aw3.18.14 was unable to detect I-A^k-$HEL_{(46-61)}$ complexes on PFA-fixed cells.

Staining and Immunofluorescence Microscopy—HEL- and LPS-treated DCs were harvested, washed twice in HBSS, and stained in suspension with unlabeled primary antibodies (Aw3.18.14 and ICAM-1), appropriate isotype controls (mouse IgG2b and rat IgG2b), and Alexa Fluor 488-labeled cholera toxin B subunit for 1 h on ice to prevent macropinocytosis of antibody. DCs not incubated with HEL were used as the appropriate control for AW3.18.14 staining. DCs were washed four times with HBSS before being fixed with 4% PFA (dissolved in 0.1 M HEPES, pH 7.4) on ice for 30 min. In some experiments, DCs were biotinylated on ice before being treated with PFA. Immediately after fixation, free PFA was quenched by washing the cells twice with 50 mM NH_4Cl in HBSS and washing once with HBSS before staining with the appropriate Alexa Fluor 546 goat anti-mouse Ig, Alexa Fluor 546 goat anti-rat Ig, or Alexa Fluor 546 streptavidin for 30 min at room temperature. Cells were washed three times with HBSS, incubated for 1 h on poly-L-lysine-coated coverslips, and mounted with Fluoromount G (SouthernBiotech). DCs were analyzed by confocal immunofluorescence microscopy using a Zeiss LSM 510 META confocal microscope, a 63× oil immersion objective lens (NA 1.4), and a pinhole diameter set to provide an optical slice thickness of 0.8 μm.

Quantitative analysis of clustering was performed using the 2.5D plot (LUT six-step) provided with the LSM 510 software as follows. A "cluster" was arbitrarily defined as a peak in pixel intensity that rises above the 2,048 (*green*) intensity value in the 2.5D plot, into the 2,730 (*red*) intensity value, and back down below the 2,048 (*green*) intensity value (see Figs. 1, 2, and 4).

Transmission Electron Microscopy—Immature DCs were incubated in medium containing 1 mg/ml HEL for 12 h and activated with LPS for 12 h, and surface proteins were biotinylated on ice. Some DCs, instead of being biotinylated, were stained on ice with mouse mAb Aw3.18.14 to detect I-A^k-$HEL_{(46-61)}$ complexes. The cells were incubated with either 15-nm colloidal gold-labeled anti-biotin antibody on ice to visualize total surface protein or 5-nm colloidal gold-labeled anti-mouse IgG on ice to detect surface I-A^k-$HEL_{(46-61)}$ complexes. The cells were allowed to adhere to Alcian blue-coated coverslips, and "plasma membrane rips" were prepared by placing each coverslip on a Formvar-coated 300-mesh copper EM grid and physically separating the coverslip/grid "sandwich" as described previously (17). EM grids were analyzed using a JEOL 100CXII transmission electron microscopy microscope.

Quantitative analysis of clustering was performed as follows. A cluster of gold particles was defined as containing at least three particles with none of the particles separated by a distance greater than 200 nm. For example, four particles all contained in a space of 80-nm diameter is defined as a single 80-nm cluster. By contrast, two particles 20 nm apart whose nearest neighbor is 190 nm away represent a single 210-nm cluster, whereas if the nearest neighbor is 210 nm away, these three particles would not represent a cluster at all. The diameter of each cluster

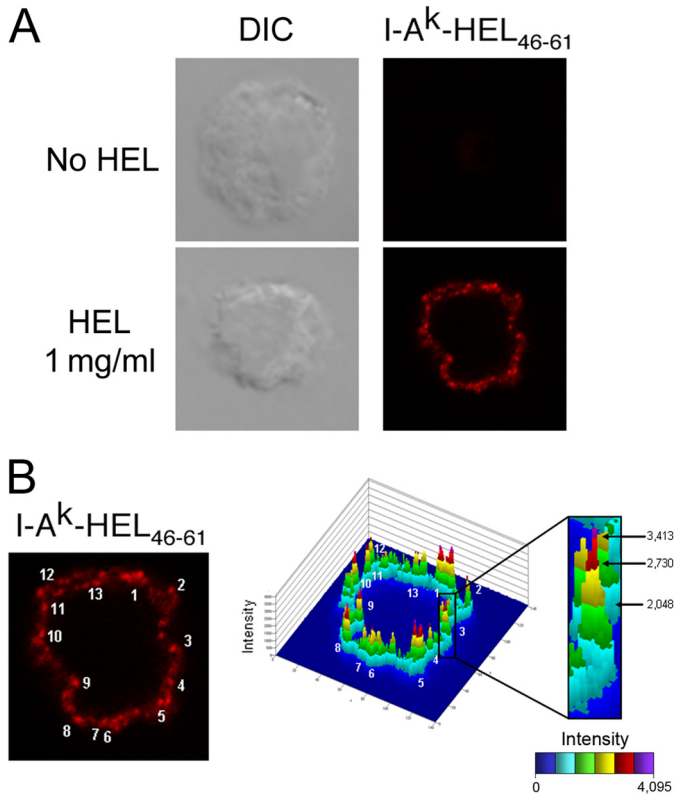

FIGURE 1. **Specific detection of I-A^k-HEL$_{(46-61)}$ complexes on the DC surface.** Immature DCs were incubated in medium alone (*no HEL*) or medium containing 1 mg/ml HEL for 12 h before being activated with LPS for 12 h. Then, DCs were stained live with mAb Aw3.18.14. *A*, differential interference contrast (*DIC*) image and I-A^k-HEL$_{(46-61)}$ (mAb Aw3.18.14) staining of a representative cell analyzed by confocal immunofluorescence microscopy. *B*, confocal images in a 0.8-μm-thick optical section were analyzed by 2.5D plot provided with the Zeiss 510 software. In this analysis, the intensity of each pixel in the field is plotted in a histogram format. A peak is defined by the criteria described under "Results." In the particular image shown, each of the 13 I-A^k-HEL$_{(46-61)}$ clusters in the image is indicated.

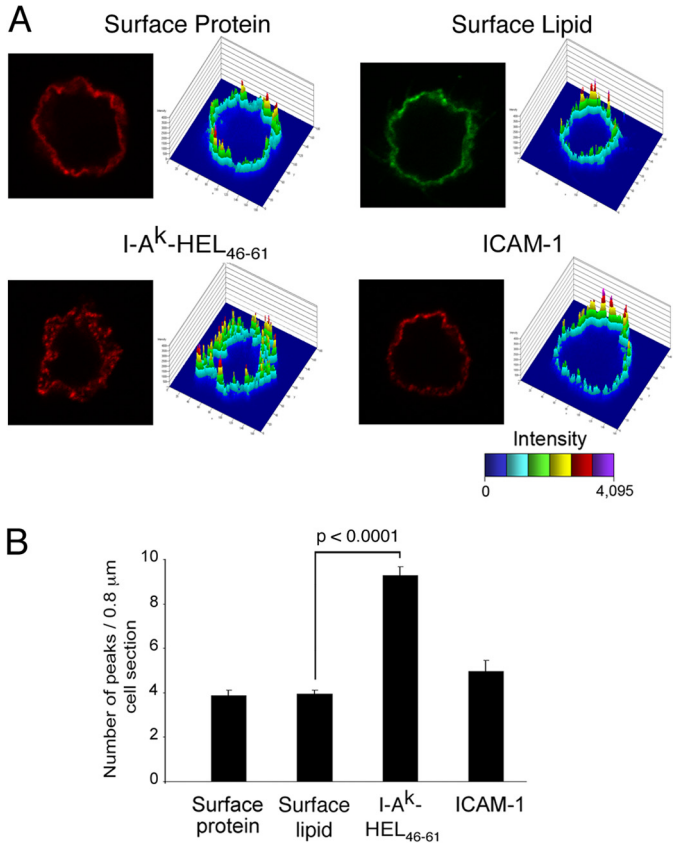

FIGURE 2. **I-A^k-HEL$_{(46-61)}$ complexes are clustered on the DC surface.** Immature DCs were incubated in medium containing 1 mg/ml HEL for 12 h, washed, and activated with LPS for 12 h, and surface proteins were then biotinylated on ice. Cells were incubated on ice with either Alexa Fluor 564-labeled avidin or Alexa Fluor 564-labeled cholera toxin to illuminate surface protein or lipid, respectively. Other cells were stained live with mAb recognizing I-A^k-HEL$_{(46-61)}$ complexes or ICAM-1 as indicated. *A*, a representative image and 2.5D plot of each stain is shown. *B*, the number of peaks visualized in each 0.8-μm-thick optical section was quantitated. The data shown are the mean ± S.D. from at least 45 individual cells from at least three independent experiments.

was determined in multiple images, and the average cluster size (in nm) was calculated. In addition, the absolute number of clusters that fell in different diameter ranges (*i.e.* 61–100 or 101–140 nm) was calculated.

T Cell Proliferation Assays—Immature DCs were treated with 1 μg/ml or 1 mg/ml HEL for 12 h. The antigen was then removed, and the cells were activated using 1 μg/ml LPS. The cells were then left untreated or incubated with MCD in HBSS for 10 min at 37 °C to extract membrane cholesterol, washed, and immediately fixed with 1% PFA in HBSS. Subsequently, and to quench free PFA, cells were washed twice with HBSS containing 100 mM glycine and resuspended in complete medium. Purified naive CD4 T cells were labeled with CFSE (5 μM) in PBS for 8 min at room temperature and washed with complete medium. PFA-fixed DCs (10^4 cells) and CFSE-labeled naive T cells (10^5 cells) were co-cultured for 2 days, and CFSE dye dilution was analyzed by FACS using a FACSCalibur flow cytometer. The percentage of CFSE-labeled T cells that underwent proliferation was calculated by FlowJo software.

RESULTS

Newly Generated pMHC-II Are Expressed on the Surface of DCs in Discrete Microclusters—The association of MHC-II with either lipid raft membrane or tetraspanin membrane microdomains plays an important role in antigen presentation (9–12, 18). Because MHC-II are directed to lipid raft microdomains in antigen-processing compartments prior to peptide loading (19), we explored the possibility that lysosomal raft association and pMHC-II transport to the plasma membrane results in the delivery of concentrated pMHC-II at the surface of the antigen-presenting cells in discrete quanta. To address this question, immature DCs were pulsed with intact HEL protein antigen and matured for 12 h with LPS to allow for the generation and transport of newly formed I-A^k-HEL$_{(46-61)}$ complexes from intracellular antigen-processing compartments out to the plasma membrane (20, 21). These complexes were detected on living DCs using mAb Aw3.18.14, an antibody that shows reactivity with I-A^k-HEL$_{(46-61)}$ complexes (14). We confirmed that this mAb has exquisite specificity for these complexes in DC and does not react with endogenous MHC-II loaded with other peptides (Fig. 1*A*). For quantitative analysis of MHC-II distribution, we used 2.5D plot software provided with the Zeiss LSM510 confocal microscope. Clusters were defined as marker density "peaks" in which surface staining was reaching a high intensity (*red step* of the 2.5D plot) and was sur-

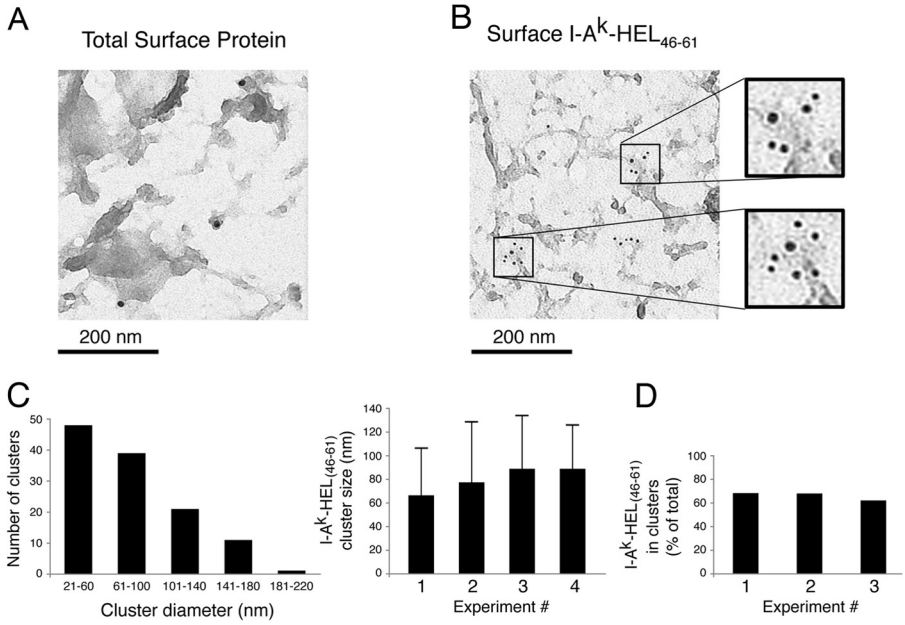

FIGURE 3. **I-A^k-HEL$_{(46-61)}$ complexes are present in 80-nm clusters on the DC surface.** Immature DCs were incubated in medium containing 1 mg/ml HEL for 12 h and activated with LPS for 12 h, and surface proteins were biotinylated on ice. The cells were also stained on ice with mouse mAb Aw3.18.14 to detect I-A^k-HEL$_{(46-61)}$ complexes. *A*, the cells were incubated with 15-nm colloidal gold-labeled anti-biotin antibody to visualize total surface protein. *B*, the cells were incubated with 5-nm colloidal gold-labeled anti-mouse Ig to detect surface I-A^k-HEL$_{(46-61)}$ complexes. *C*, the absolute number of clusters observed that had diameters in the indicated range from four independent experiments was determined. In addition, the mean I-A^k-HEL$_{(46-61)}$ cluster size ± S.D. from four different experiments was quantitated as described under "Experimental Procedures." *D*, the number of colloidal gold anti-I-A^k-HEL$_{(46-61)}$ particles present within <200-nm clusters was determined and was expressed as a fraction of the total amount of gold particles present in three independent experiments (>125 total gold particles/experiment).

rounded by low intensity (*green step* of the 2.5D plot; Fig. 1*B*). By this definition, the cell shown in Fig. 1*B* has 13 I-A^k-HEL$_{(46-61)}$ clusters per 0.8-μm cell section.

The goal of our study is to examine the plasma membrane distribution of newly arrived I-A^k-HEL$_{(46-61)}$ complexes; however, the plasma membrane of DCs is characterized by the presence of numerous veils and microvilli (22) that make a "regular" membrane appear irregular even by confocal microscopy. To exclude the possibility that high local densities of proteins of interest were due to their presence in these membrane folds, we also analyzed the distribution of all plasma membrane proteins (by biotin labeling the DC surface) as well as plasma membrane glycolipid (by staining for the ganglioside GM1). Clusters analysis revealed that total surface proteins and surface lipids showed a relatively homogeneous distribution (Fig. 2) with an average of 4 peaks per 0.8-μm cell section. This "background" value likely represents the number of membrane veil/microvilli concentrations present in each confocal section. The distribution of the cell surface adhesion molecule ICAM-1 (which is excluded from plasma membrane microdomains (19)) was comparable with that of total membrane protein or lipid and was not enriched in clusters (Fig. 2). By contrast, those I-A^k-HEL$_{(46-61)}$ complexes that had inserted into the plasma membrane during the 12-h activation period with LPS had a dramatically clustered phenotype, with an average of nine clusters observed per cell section. Very similar results were obtained when HEL-pulsed DCs were activated with LPS for either 12 h or 30 h (supplemental Fig. 1), revealing that the I-A^k-HEL$_{(46-61)}$ microclusters are relatively stable structures.

We also analyzed the distribution of total biotinylated surface proteins and newly arrived I-A^k-HEL$_{(46-61)}$ complexes on native plasma membranes of DCs using immunoelectron microscopy (17). In agreement with our results obtained by confocal microscopy analysis, colloidal gold-labeled streptavidin revealed a relatively homogeneous distribution of biotinylated surface proteins on plasma membrane rips of DCs (Fig. 3*A*). By contrast, the immunogold labeling with mAb Aw3.18.14 revealed a distribution of I-A^k-HEL$_{(46-61)}$ complexes that was preferentially in clusters (Fig. 3*B*). Most of these clusters showed a diameter between 21 and 100 nm (73% of all clusters measured) with an average cluster diameter of 81 ± 10 nm (Fig. 3*C*). Furthermore, quantitative analysis of immunogold distribution showed that more than 60% of all I-A^k-HEL$_{(46-61)}$ complexes resided in <200-nm clusters (Fig. 3*D* and supplemental Fig. 2). Taken together, these data demonstrate that MHC-II are distributed on the surface of DC in clusters and that newly generated pMHC-II are present on the plasma membrane in a highly clustered distribution.

Plasma Membrane pMHC-II Clustering Is Cholesterol-dependent—MHC-II associate with cholesterol-dependent lipid raft membrane microdomains (23) during intracellular transport, and we therefore set out to determine whether depletion of plasma membrane cholesterol affected the structural integrity of I-A^k-HEL$_{(46-61)}$ surface clusters. Plasma membrane cholesterol was extracted using methyl-β-cyclodextrin (MCD), a cyclic carbohydrate that has been shown to remove cholesterol and disrupt lipid raft integrity (24, 25). HEL-pulsed and LPS-matured DCs were treated with MCD for 10 min immediately prior to analysis. Quantitative analysis of plasma membrane cholesterol content revealed that MCD treatment reduced surface cholesterol levels by 32 ± 4% (Fig. 4*A*). Cluster analysis by confocal microscopy revealed that reducing plasma

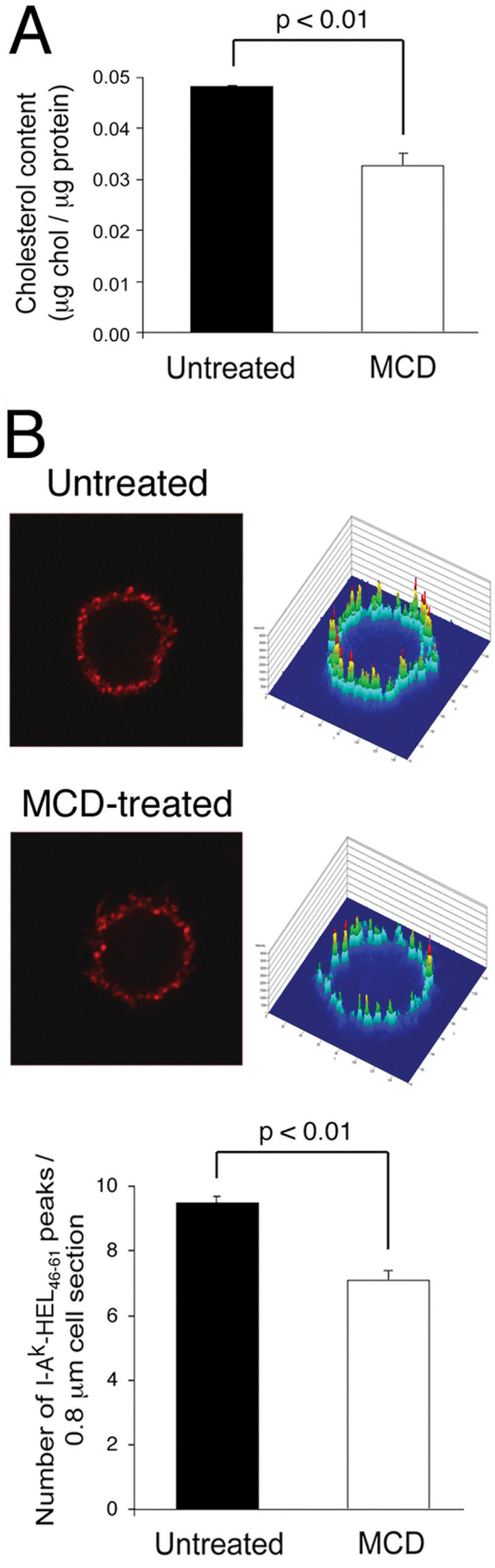

FIGURE 4. **Cholesterol depletion reduces I-A^k-HEL$_{(46-61)}$ clustering on the DC surface.** DCs pulsed for 12 h with HEL and activated by incubation with LPS for 12 h were untreated or treated with 10 mM MCD for 10 min at 37 °C. *A*, the cholesterol content of the cells (μg of cholesterol/μg of total protein) after the 10-min incubation was determined, and the mean ± S.D. from three independent experiments is shown. *B*, the cells were stained on ice with mAbs recognizing I-A^k-HEL$_{(46-61)}$ complexes and analyzed by confocal immunofluorescence microscopy and 2.5D plot analysis as in Fig. 1. Representative images of untreated and MCD-treated DCs are shown. The number of peaks visualized in each 0.8-μm thick optical section was quantitated. The data shown are the mean ± S.D. from at least 45 individual cells in three independent experiments.

membrane cholesterol significantly reduced the clustering of I-A^k-HEL$_{(46-61)}$ complexes without changing the appearance of individual clusters (Fig. 4*B*). It should also be noted that membrane cholesterol depletion was far from complete under the experimental conditions used and that DCs remained viable in all experiments, and therefore any observed effects likely underestimate the actual importance of membrane cholesterol in I-A^k-HEL$_{(46-61)}$ clustering.

Disruption of pMHC-II Clusters Preferentially Inhibits APC Function under Conditions of Low Antigen Dose—The integrity of plasma membrane lipid rafts was important for the ability of B cells and DCs to activate CD4 T cells (9–12). In an attempt to determine whether cholesterol-dependent clustering of I-A^k-HEL$_{(46-61)}$ complexes is important for APC function under conditions in which I-A^k-HEL$_{(46-61)}$ complexes are limiting, we incubated DCs with different amounts of HEL protein prior to LPS activation and cholesterol depletion. FACS analysis confirmed our previous findings (9) that reducing plasma membrane cholesterol with MCD did not reduce that absolute amount of I-A^k-HEL$_{(46-61)}$ complexes present on the cell surface (Fig. 5*A*). MCD treatment had only a modest effect on the ability of DCs to induce HEL-specific T cells to proliferate when the DCs were pulsed with a large amount of antigen (Fig. 5, *B* and *C*). By contrast, when the DCs were pulsed with 1,000 times less HEL, MCD treatment dramatically inhibited the ability of the DCs to stimulate the T cells. Taken together, these data demonstrate that plasma membrane cholesterol depletion disrupts the association of newly generated pMHC-II in membrane clusters and preferentially inhibits the ability of DCs to stimulate antigen-specific T cells under conditions of limiting antigen dose.

DISCUSSION

Although APCs such as DCs express large numbers of MHC-II on their cell surface, the absolute amount of any given specific pMHC-II expressed on the DC surface is quite small (7, 8, 26). Despite this fact, DCs very efficiently stimulate naive CD4 T cells. We have previously shown that nascent MHC-II associate with cholesterol/sphingolipid-rich lipid raft microdomains in intracellular antigen-processing compartments (19), leading us to propose that intracellular peptide binding and lipid raft association generate quanta of specific pMHC-II that are locally concentrated and efficiently recognized by TCRs on antigen-specific CD4 T cells (23). By using an I-A^k-HEL$_{(46-61)}$-specific mAb to monitor expression of MHC-II-HEL antigen complexes, we now show that specific pMHC-II that are generated intracellularly are deposited on the cell surface after maturation and are distributed in discrete microclusters on the DC plasma membrane. Our data are in excellent agreement with the data of Turley *et al.* (20) who found that newly generated pMHC-II appeared clustered on the maturing DC surface and that these clusters also contained the costimulatory protein

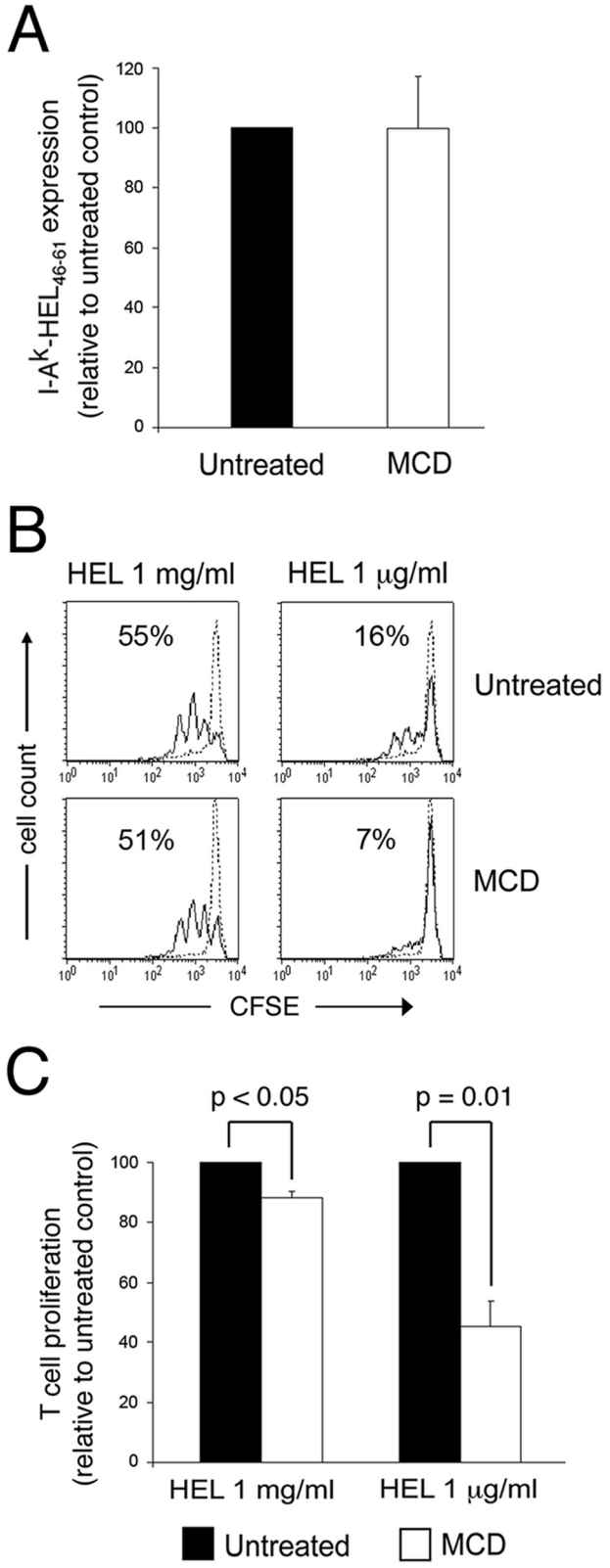

FIGURE 5. **Cholesterol depletion preferentially inhibits T cell activation under conditions of limiting antigen dose.** Immature DCs were incubated in medium containing either 1 mg/ml HEL or 1 μg/ml HEL for 12 h, washed, and activated with LPS for 12 h. The cells were then untreated or treated with 10 mM MCD for 10 min at 37 °C, washed, and immediately fixed with PFA. *A*, the expression of I-A^k-HEL$_{(46-61)}$ complexes on the cells was examined by FACS analysis using the I-A^k-HEL$_{(46-61)}$ complex-specific mAb C4H3. The mean fluorescence intensity of C4H3 staining on MDC-treated cells was expressed as a percentage of that on untreated cells. The data shown are the mean ± S.D. from three independent experiments. *B* and *C*, the ability of the DCs to induce the proliferation of CFSE-labeled naive HEL-specific CD4 T cells was determined. *B*, representative histogram showing CFSE dilution of naive CD4 T cells after incubation with each DC subset is shown. *C*, the effect of MCD on CD4 T cell activation by HEL-loaded DCs treated was determined and is expressed relative to the extent of T cell proliferation from untreated DCs. The data shown are the mean ± S.D. from five independent experiments.

CD86. Consistent with the hypothesis that these clusters arise from the insertion of antigen-processing compartment-derived raft domains into the plasma membrane, we find that cholesterol sequestration and raft disruption dramatically reduce the clustered distribution of pMHC-II on the plasma membrane of DCs.

The formation of an immunological synapse between an antigen-specific T cell and an antigen-bearing APC is critical to efficient T cell activation (1). Our data showing that pMHC-II microclusters are important for T cell interactions with APCs fit well with data demonstrating that microclusters of TCRs at the immunological synapse act as scaffolds for T cell signaling (27, 28). Indeed, these TCR microclusters eventually coalesce into the central supramolecular activation cluster ((29)) on the T cell side of the immunological synapse (27, 28). It is interesting to note that antigen-specific pMHC-II are also concentrated at the central supramolecular activation cluster on the APC (10), and we propose that in analogy with the TCR, the pMHC-II at the central supramolecular activation cluster arise from coalescence of specific pMHC-II microclusters driven by TCR interactions.

The effect of cluster disruption on APC function is profound, and cluster-disrupted DCs are poor stimulators of naive antigen-specific CD4 T cells. The disruption of APC function by cholesterol depletion is not absolute, however, because the importance for clustering can be overcome if the DCs are loaded with a large amount of HEL protein antigen (which gives rise to large amounts of I-A^k-HEL$_{(46-61)}$ complexes on the DC surface). This finding is interpreted quite simply. In cells possessing large amounts of specific pMHC-II on their surface, the requirement for *local* concentration of pMHC-II (in microdomains) is diminished because the absolute density of specific pMHC-II is great. By contrast, under conditions of low antigen dose, microclusters are important because the absolute amount of specific pMHC-II/cell is very low, and it is only by their association with microclusters that a local density of specific pMHC-II high enough for T cell activation can be achieved. Unfortunately, due to antibody sensitivity issues, it was not possible to actually visualize the distribution of the very small amounts of I-A^k-HEL$_{(46-61)}$ complexes generated under the conditions of low antigen dose used in this study. Because activating DCs transiently increase macropinocytosis to increase foreign antigen uptake (5) and because the initial association of MHC-II with lipid raft microdomains occurs in antigen-processing compartments (19), it is likely that the microclusters that are deposited in the plasma membrane of DCs are not only clustered for more efficient T cell activation but are enriched for MHC-II-foreign peptide complexes that will enhance T cell activation even further.

Acknowledgments—We thank Lisa Drake for assistance with transmission microscopy analysis and Michael Kruhlak for assistance with confocal immunofluorescence microscopy analysis.

REFERENCES

1. Krogsgaard, M., and Davis, M. M. (2005) How T cells 'see' antigen. *Nat. Immunol.* **6,** 239–245
2. Trombetta, E. S., and Mellman, I. (2005) Cell biology of antigen processing *in vitro* and *in vivo*. *Annu. Rev. Immunol.* **23,** 975–1028
3. Boes, M., Cerny, J., Massol, R., Op den Brouw, M., Kirchhausen, T., Chen, J., and Ploegh, H. L. (2002) T-cell engagement of dendritic cells rapidly rearranges MHC class II transport. *Nature* **418,** 983–988
4. Chow, A., Toomre, D., Garrett, W., and Mellman, I. (2002) Dendritic cell maturation triggers retrograde MHC class II transport from lysosomes to the plasma membrane. *Nature* **418,** 988–994
5. West, M. A., Wallin, R. P., Matthews, S. P., Svensson, H. G., Zaru, R., Ljunggren, H. G., Prescott, A. R., and Watts, C. (2004) Enhanced dendritic cell antigen capture via Toll-like receptor-induced actin remodeling. *Science* **305,** 1153–1157
6. Young, L. J., Wilson, N. S., Schnorrer, P., Proietto, A., ten Broeke, T., Matsuki, Y., Mount, A. M., Belz, G. T., O'Keeffe, M., Ohmura-Hoshino, M., Ishido, S., Stoorvogel, W., Heath, W. R., Shortman, K., and Villadangos, J. A. (2008) Differential MHC class II synthesis and ubiquitination confers distinct antigen-presenting properties on conventional and plasmacytoid dendritic cells. *Nat. Immunol.* **9,** 1244–1252
7. Harding, C. V., and Unanue, E. R. (1990) Quantitation of antigen-presenting cell MHC class II/peptide complexes necessary for T-cell stimulation. *Nature* **346,** 574–576
8. Demotz, S., Grey, H. M., and Sette, A. (1990) The minimal number of class II MHC-antigen complexes needed for T cell activation. *Science* **249,** 1028–1030
9. Anderson, H. A., Hiltbold, E. M., and Roche, P. A. (2000) Concentration of MHC class II molecules in lipid rafts facilitates antigen presentation. *Nat. Immunol.* **1,** 156–162
10. Hiltbold, E. M., Poloso, N. J., and Roche, P. A. (2003) MHC class II-peptide complexes and APC lipid rafts accumulate at the immunological synapse. *J. Immunol.* **170,** 1329–1338
11. Gombos, I., Detre, C., Vámosi, G., and Matkó, J. (2004) Rafting MHC-II domains in the APC (presynaptic) plasma membrane and the thresholds for T-cell activation and immunological synapse formation. *Immunol. Lett.* **92,** 117–124
12. Eren, E., Yates, J., Cwynarski, K., Preston, S., Dong, R., Germain, C., Lechler, R., Huby, R., Ritter, M., and Lombardi, G. (2006) Location of major histocompatibility complex class II molecules in rafts on dendritic cells enhances the efficiency of T-cell activation and proliferation. *Scand. J. Immunol.* **63,** 7–16
13. Inaba, K., Inaba, M., Romani, N., Aya, H., Deguchi, M., Ikehara, S., Muramatsu, S., and Steinman, R. M. (1992) Generation of large numbers of dendritic cells from mouse bone marrow cultures supplemented with granulocyte/macrophage colony-stimulating factor. *J. Exp. Med.* **176,** 1693–1702
14. Dadaglio, G., Nelson, C. A., Deck, M. B., Petzold, S. J., and Unanue, E. R. (1997) Characterization and quantitation of peptide-MHC complexes produced from hen egg lysozyme using a monoclonal antibody. *Immunity* **6,** 727–738
15. Zhong, G., Reis e Sousa, C., and Germain, R. N. (1997) Production, specificity, and functionality of monoclonal antibodies to specific peptide-major histocompatibility complex class II complexes formed by processing of exogenous protein. *Proc. Natl. Acad. Sci. U.S.A.* **94,** 13856–13861
16. Furuta, K., Ishido, S., and Roche, P. A. (2012) Encounter with antigen-specific primed CD4 T cells promotes MHC class II degradation in dendritic cells. *Proc. Natl. Acad. Sci. U.S.A.* **109,** 19380–19385
17. Caballero, A., Katkere, B., Wen, X. Y., Drake, L., Nashar, T. O., and Drake, J. R. (2006) Functional and structural requirements for the internalization of distinct BCR-ligand complexes. *Eur. J. Immunol.* **36,** 3131–3145
18. Kropshofer, H., Spindeldreher, S., Röhn, T. A., Platania, N., Grygar, C., Daniel, N., Wölpl, A., Langen, H., Horejsi, V., and Vogt, A. B. (2002) Tetraspan microdomains distinct from lipid rafts enrich select peptide-MHC class II complexes. *Nat. Immunol.* **3,** 61–68
19. Poloso, N. J., Muntasell, A., and Roche, P. A. (2004) MHC class II molecules traffic into lipid rafts during intracellular transport. *J. Immunol.* **173,** 4539–4546
20. Turley, S. J., Inaba, K., Garrett, W. S., Ebersold, M., Unternaehrer, J., Steinman, R. M., and Mellman, I. (2000) Transport of peptide-MHC class II complexes in developing dendritic cells. *Science* **288,** 522–527
21. Inaba, K., Turley, S., Iyoda, T., Yamaide, F., Shimoyama, S., Reis e Sousa, C., Germain, R. N., Mellman, I., and Steinman, R. M. (2000) The formation of immunogenic major histocompatibility complex class II-peptide ligands in lysosomal compartments of dendritic cells is regulated by inflammatory stimuli. *J. Exp. Med.* **191,** 927–936
22. Fisher, P. J., Bulur, P. A., Vuk-Pavlovic, S., Prendergast, F. G., and Dietz, A. B. (2008) Dendritic cell microvilli: a novel membrane structure associated with the multifocal synapse and T-cell clustering. *Blood* **112,** 5037–5045
23. Poloso, N. J., and Roche, P. A. (2004) Association of MHC class II-peptide complexes with plasma membrane lipid microdomains. *Curr. Opin. Immunol.* **16,** 103–107
24. Keller, P., and Simons, K. (1998) Cholesterol is required for surface transport of influenza virus hemagglutinin. *J. Cell Biol.* **140,** 1357–1367
25. Ilangumaran, S., and Hoessli, D. C. (1998) Effects of cholesterol depletion by cyclodextrin on the sphingolipid microdomains of the plasma membrane. *Biochem. J.* **335,** 433–440
26. Reay, P. A., Matsui, K., Haase, K., Wulfing, C., Chien, Y. H., and Davis, M. M. (2000) Determination of the relationship between T cell responsiveness and the number of MHC-peptide complexes using specific monoclonal antibodies. *J. Immunol.* **164,** 5626–5634
27. Campi, G., Varma, R., and Dustin, M. L. (2005) Actin and agonist MHC-peptide complex-dependent T cell receptor microclusters as scaffolds for signaling. *J. Exp. Med.* **202,** 1031–1036
28. Yokosuka, T., Sakata-Sogawa, K., Kobayashi, W., Hiroshima, M., Hashimoto-Tane, A., Tokunaga, M., Dustin, M. L., and Saito, T. (2005) Newly generated T cell receptor microclusters initiate and sustain T cell activation by recruitment of Zap70 and SLP-76. *Nat. Immunol.* **6,** 1253–1262
29. Monks, C. R., Freiberg, B. A., Kupfer, H., Sciaky, N., and Kupfer, A. (1998) Three-dimensional segregation of supramolecular activation clusters in T cells. *Nature* **395,** 82–86